Pharmaceutical Research, Vol. 24, No. 2, February 2007 (© 2006)
DOI: 10.1007/s11095-006-9161-8

Research Paper

Interaction of Omeprazole with a Methylated Derivative of β-Cyclodextrin: Phase Solubility, NMR Spectroscopy and Molecular Simulation

Ana Figueiras,[1] J. M. G. Sarraguça,[2] Rui A. Carvalho,[3] A. A. C. C. Pais,[2] and Francisco J. B. Veiga[1,4]

Received July 10, 2006; accepted September 5, 2006; published online December 20, 2006

Purpose. Cyclodextrins are known to be good solubility enhancers for several drugs, improving bioavailability when incorporated in pharmaceutical formulations. In this work we intend to assess and characterize the formation of inclusion complexes between omeprazole (OME) and a methylated derivative of β-cyclodextrin, methyl-β-cyclodextrin (MβCD). A comparison with results obtained from the most commonly used natural cyclodextrin, β-cyclodextrin (βCD) is also presented in most cases.
Materials and Methods. The interaction of OME with the mentioned cyclodextrins in aqueous solutions was studied by phase solubility studies, 1D ^{1}H and 2D rotating frame nuclear overhauser effect NMR spectroscopy (ROESY) and Molecular Dynamics.
Results. The solubility of OME was significantly increased by formation of inclusion complexes with each cyclodextrin. Phase solubility studies and continuous variation plots revealed that OME forms an inclusion complex in a stoichiometry of 1:1 with both cyclodextrins. ^{1}H NMR and ROESY spectra of the inclusion complexes indicated that the benzimidazole moiety is included within the cyclodextrins cavities. Molecular dynamics showed that OME is more deeply included in the MβCD than in βCD cavity, in agreement with a larger apparent stability constant (K_S) obtained for the inclusion complex with MβCD.
Conclusions. MβCD proved to be an efficient enhancer of OME solubility, thus possessing characteristics for being an useful excipient in pharmaceutical formulations of this drug.

KEY WORDS: cyclodextrin; inclusion complex; molecular dynamics; NMR spectroscopy; omeprazole; phase solubility studies.

INTRODUCTION

Omeprazole is a potent reversible inhibitor of the gastric proton pump H^+/K^+-ATPase. The molecular structure of OME, illustrated in Fig. 1a, is composed of a substituted pyridine ring linked to a benzimidazole by a sulfoxide chain (1). Omeprazole is only slightly soluble in water, but is highly soluble in alkaline solutions as the negatively charged ion. It is an ampholyte with pKa = 4 (pirydinium ion) and 8.8 (benzimidazole). In solution OME degrades rapidly at low pH values (2) and it is photo and heat sensitive (3).

Drug solubility and stability are two very important factors with respect to drug administration and drug delivery. The potential use of natural cyclodextrins and their synthetic derivatives for improvement of the solubility, stability and/or bioavailability by formation of inclusion complexes with drugs has been extensively studied (4,5).

Cyclodextrins are cyclic organic compounds obtained by enzymatic transformation of starch. Among this class of "host" molecules, the β-cyclodextrin is one of the most abundant natural oligomers and corresponds to the association of seven glucose units exhibiting a cavity with a hydrophobic character whereas the exterior is strongly hydrophilic. This peculiar structure allows guest molecules to be included into the cavity via non-covalent bonds to form inclusion complexes (6).

Natural cyclodextrins have limited water solubility. However, a significant increase in water solubility has been obtained by alkylation of the free hydroxyl groups of the cyclodextrins resulting in hydroxyalkyl, methyl, and sulfobutyl derivatives. The ability of cyclodextrins to form inclusion complexes may also be enhanced by substitution on the hydroxyl groups (see, for example, (7)). For several years, modified cyclodextrins have been used as solubilizing agents being the most important among the industrially produced βCD derivatives, the highly water-soluble methylated and hydroxypropylated βCDs.

The most widely used approach to study inclusion complexation is the phase solubility method described by Higuchi and Connors (8) which examines the effect of a solubilizer or ligand (cyclodextrin) on the drug being

[1] Laboratory of Pharmaceutical Technology, Faculty of Pharmacy, University of Coimbra, 3000-295, Coimbra, Portugal.
[2] Department of Chemistry, Faculty of Sciences and Technology, University of Coimbra, Coimbra, Portugal.
[3] NMR Spectroscopy Center, Department of Biochemistry, Faculty of Sciences and Technology, University of Coimbra, Coimbra, Portugal.
[4] To whom correspondence should be addressed. (e-mail: fveiga@ci.uc.pt)

solubilized (the substrate). Phase solubility diagrams are categorized into A and B types; A type curves indicate the formation of soluble inclusion complexes while B type suggest the formation of inclusion complexes with poor solubility (9).

^{1}H NMR spectroscopy represents one of the most powerful tools for describing supramolecular assemblies in the liquid state. Chemical shift variations ($\Delta\delta$) of specific host or guest nucleus can provide evidence for the formation of inclusion complexes in solution, since significant changes in microenvironment are known to occur between the free and bound states. A detailed picture of the geometry of the host–guest complex in solution can be obtained by the application of NMR advanced techniques such as ROESY experiments (6,10). The information obtained allows the calculation of the stoichiometry and stability constant of the complex as well as the confirmation of complex formation and specially the orientation of the guest molecule in the cyclodextrin cavity (11). Due to this uniqueness of the NMR data, it has been adopted as a routine tool for the study of host–guest supramolecular chemistry and there are now hundreds of reports where NMR titration was used to measure intermolecular association (12–14).

A large variety of computer simulation techniques have been used in the last years to study structural and energetic properties of cyclodextrins (15–17) and cyclodextrin inclusion complexes (18–21) in aqueous solutions, giving a general insight over a number of aspects of such systems. In this study, Molecular Dynamics simulations were carried out to clarify and characterize different aspects of the dynamics of complex formation as well as structural aspects of the complexes formed with OME.

The purpose of this study is to assess and characterize the formation of an inclusion complex between OME and MβCD (Fig. 1b). In addition, βCD, the natural cyclodextrin, was included in the study in order to analyze the influence of the hydrophobic character in the inclusion of guest molecules in the CD cavity. The study presented here is composed by phase solubility studies, ^{1}H NMR spectroscopy and molecular simulation.

MATERIALS AND METHODS

Materials

β-cyclodextrin (βCD, MW=1135) and methyl-β-cyclodextrin (MβCD, MW=1190 and an average degree of substitution, DS = 0.5) were kindly donated by Roquette (Lestrem, France) and OME was kindly donated by Belmac Laboratory, S.A. (Barcelona, Spain). Deuterium oxide (D_2O; 99.97%) and NaOD were purchased from Euriso-top (Peypin, France) and Sigma Aldrich (Madrid, Spain), respectively. All other reagents were of the highest purity available from commercial sources.

Phase Solubility Studies

Phase solubility studies were carried out at room temperature (21 ± 1°C) following the method of Higuchi and Connors (8). Excess amounts of OME were weighed in glass flasks to which 10 ml of boric/borate buffer pH=10 (22) were added. These flasks contained increasing amounts of βCD (0–1.5%, w/v) or MβCD (0–5%, w/v). Glass containers were sealed and mechanically stirred, protected from light until reaching the equilibrium (about 96 h). All suspensions were filtered through a 0.45 μm membrane filter (Millipore) and analyzed spectrophotometrically (UV-1603, Shimadzu, Japan) at 305.5 nm.

The apparatus was calibrated with the corresponding blank for each assay and three replicates were made. The presence of cyclodextrin did not interfere with the spectrophotometric assay of OME.

Stability constants (K_S) were calculated from the phase solubility diagrams using the equation:

$$K_s = \text{slope}/S_0\,(1 - \text{slope}) \quad (1)$$

where S_0 is OME solubility in the absence of βCD or MβCD (intercept).

^{1}H NMR Studies

^{1}H NMR spectra were recorded at 25°C on a Varian 500 MHz spectrometer using a 5 mm NMR probe. The NMR spectra were acquired with solvent presaturation. Acquisition parameters consisted of 24k points covering a sweep width of 8 kHz, a pulse width of 18 μs and a total repetition time of 15 s. Digital zero filling to 64k and a 0.5 Hz exponential were applied before Fourier Transformation. The resonance at 4.681 ppm due to residual solvent (HOD) was used as the internal reference. Samples were prepared by dissolving an amount of the solid complex, previously prepared by the lyophilized method (23), in D_2O to achieve an OME concentration of 6 mM in the case of βCD and 15 mM in the complex formed with MβCD. Reference samples containing pure OME (6 and 15 mM), βCD (6 mM) and MβCD (15 mM) were also prepared. The final pH was adjusted to 10.0 ± 0.1, in all samples, in order to minimize the degradation and increase the solubility of OME. ^{1}H NMR chemical shifts variations ($\Delta\delta$) were calculated according to the formula:

$$\Delta\delta = \delta(\text{complex}) - \delta(\text{free}). \quad (2)$$

The continuous variation method (Job plot) was adopted to determine the stoichiometry of the complexes formed. A series of mixtures of OME with each cyclodextrin were made. In each of these the sum of the concentrations of the two species was kept constant at 6 mM but the mol fraction of each component, m and n for OME and cyclodextrin respectively, were varied (19) according to $r = n/(m + n)$.

ROESY Experiments

ROESY spectra were acquired in the phase sensitive mode with solvent presaturation using the same spectrometer. Each spectrum consisted of a matrix of 2048 (F2) by 1024 (F1) covering a sweep width of 4000 Hz. Spectra were obtained on the lyophilized samples having a 1:1 OME/cyclodextrin ratio, using spin-lock mixing periods of 300 ms. A 300 ms mixing time was chosen after careful calibration for each of the supramolecular complexes under consideration. Other mixing periods (e.g., 150, 500 and 750 ms) were used

but the 300 ms period was the one that simultaneously provided the best intra- and intermolecular NOE correlations. Before Fourier transformation, the matrix was zero filled to 4096 (F2) by 2048 (F1) and Gaussian apodization functions were applied in both dimensions.

The extent and the direction of the inclusion in the cyclodextrin cavity were observed by the detection of intermolecular nuclear Overhauser effects (NOEs) between OME and cyclodextrins.

Molecular Simulation

Molecular Dynamics studies were performed using the GROMACS package and employing the GROMACS ffgmx force field (24,25).

An initial guess for the OME molecule was produced, while the βCD structure was originally obtained from the HIC-Up on-line database (26). The MβCD was obtained by editing the original βCD structure and adding the desired substitution groups. Considering the degree of substitution of the MβCD used experimentally and the larger reactivity of the oxygens in position 6 in respect to oxygens in position 2 and 3 of βCD (27), three methyl groups were added to oxygens on position 6 of βCD (Fig. 1b). The structures were converted to GROMACS input files (conformation and topology) using PRODRG (28).

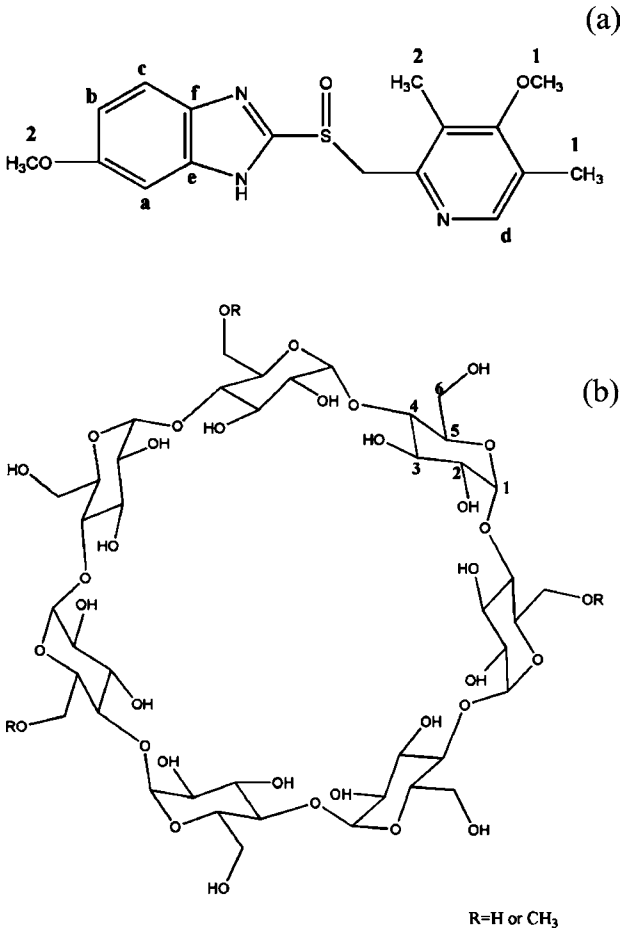

Fig. 1. Chemical structure of omeprazole (a) and β-cyclodextrin (R=H)/methyl-β-cyclodextrin (R=CH_3) (b).

The model system aims to reproduce the conditions used in the experimental section. The OME molecule at pH=10 is in the benzimidazole deprotonated form (29,30). The deprotonated form of OME was obtained by extracting the benzimidazole proton when running PRODRG and setting the partial charges on the molecule according to the charge distributions obtained from GAMESS (31) at the pm3 level, for the protonated and deprotonated forms. The minimized energy structures obtained from GAMESS and GROMACS in the gas phase for the protonated forms presented differences in bond length smaller than 0.05 Å.

The electroneutrality of the systems containing OME is maintained by the introduction of one sodium ion. The long range electrostatic interactions are handled by particle-mesh Ewald method (32). The solvent is considered explicitly using the SPC water model and an algorithm for rigid water molecules (33). The system is enclosed in a cell with periodic boundary conditions. For the systems where OME and each cyclodextrin are present, a box with an approximate volume of $39\times37\times33$ $Å^3$ is used containing approximately 1,565 water molecules. In the remaining systems, the box volume is of approximately $35\times32\times28$ $Å^3$, with more than 980 water molecules. The simulation is conducted in the NPT ensemble at constant temperature, T=300 K, and pressure, P=1 atm, with coupling to an external bath (34).

An equilibration run of at least 2 ns was done previous to the production trajectory runs, using a timestep of 2 fs, with constraints in all bonds (35). The formation of the inclusion complex is a result of the equilibration process and equilibration was only considered to be completed once inclusion is observed. The production runs were carried out for at least 7.5 ns with a timestep not exceeding 2.0 ps. A second production run of the same dimension of the first one was done on the systems where only cyclodextrins are present in solution starting from the last conformation of the first production run to evaluate the possibility of other conformations to occur.

GAMESS was also used in order to assess the conformational stability of different conformation types attained by βCD and MβCD when alone in water. The first and last conformations of the trajectory of the production runs were used to calculate, at the pm3 level, the corresponding gas phase optimized structures.

RESULTS AND DISCUSSION

Phase Solubility Studies

The phase solubility study of OME with MβCD is shown in Fig. 2. OME solubility increases linearly with cyclodextrin concentration and the slope is smaller than unity, over the entire concentration range studied, indicating an A_L type diagram with the formation of a complex with 1:1 stoichiometry.

The estimated K_S of the inclusion complexes, the OME solubility in borate buffer (S_0), the OME solubility in cyclodextrin solutions (S_2) and the corresponding slopes are presented in Table I. The OME solubility presents, approximately, a 1.7 and 3.4 fold increase in the presence of βCD and MβCD, respectively, in comparison with S_0. This corresponds to a 1.9 fold increase in solubility of OME in

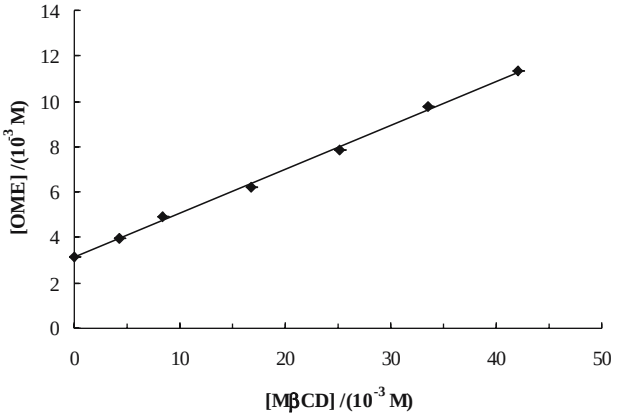

Fig. 2. Phase solubility studies of OME as a function of MβCD concentrations. Each *point* represents the mean of three determinations. Error bars are smaller than symbols.

the presence of MβCD when comparing to the solubility in the presence of βCD.

The K_S of the inclusion complexes determined in this work are 57 and 77 M^{-1} for βCD and MβCD, respectively, suggesting that MβCD forms a more stable inclusion complex with OME than βCD. The K_S of the inclusion complex OME with other modified βCD (2-hydroxypropyl-β-cyclodextrin) has been determined by other authors (36). The value obtained is of the same magnitude, $K_S = 69$ M^{-1}, but smaller than the one found for the OME:MβCD inclusion complex.

The low magnitude of the constants obtained indicates a weak interaction between the drug and the cyclodextrins used in this study. In fact at pH=10, in order to stabilize the OME, the drug is in the ionized form but ionization of the drug molecules greatly reduces the complexation or magnitude of the K_S for the complexes formed. Ionized forms of drug molecules are more hydrophilic, thus having less propensity to form an inclusion complex by displacing water molecules from the cyclodextrin cavity (37,38). However, ionization is a common method for increasing the aqueous solubility of ionizable drugs and, in aqueous solutions, cyclodextrin complexation of ionized drug molecules can result in larger total drug solubilization, i.e., the solubilization of a drug both due to ionization and inclusion in the cavity (39).

^{1}H NMR Spectroscopy

In the present work, ^{1}H NMR spectroscopy measurements were performed to elucidate the structure of OME:MβCD inclusion complex. In the presence of the drug, an appreciably upfield shift for H-3 and H-5 was observed (see Table II) in the MβCD spectra, which demonstrated a clear involvement of these protons in host–guest interactions. The order of the upfield shifts was found to be $H_5(\Delta\delta/\text{ppm}=-0.086)>H_3(\Delta\delta/\text{ppm}=-0.054)$. Since both H-3 and H-5 protons are located in the interior of the MβCD cavity, and H-3 protons are near the wide side while H-5 protons are near the narrow side, such order of upfield shifts suggests that either the entrance of the drug is made by the narrow side of the cavity or that there is a very deep penetration of the drug into the CD cavity but with an entrance by the wide side. Such interaction is also suggested by the observed upfield shifts for H-6 protons. All the exterior protons of MβCD were influenced and we cannot exclude the existence of interactions with the external surface of the cavity, that could be ascribed to hydrophobic interactions with methyl groups at the edge of the MβCD cavity and the guest molecule (23).

The δ and corresponding $\Delta\delta$ values for OME protons in the native and complexed states are reported in Table III. In the benzimidazole moiety, we observe upfield shifts in the Ha, Hb, Hc protons and methoxy 2 group with similar magnitude ($\Delta\delta=-0.025$, -0.036, -0.024 and -0.026), suggesting a total inclusion of this moiety in the MβCD cavity. We have observed similar but smaller upfield shifts when OME is complexed with βCD (data not shown). These upfield shifts are generally attributed to a shielding effect induced by the nuclei on the inner surface of βCD complexes (40) and indicate that these protons are close to a host atom which is rich in π-electrons. In this case such effects are associated with oxygen atoms, and also reflect conformational changes produced by the inclusion phenomenon (23). Similarly to βCD, in the pyridinic moiety the pronounced upfield shift experienced only by the methoxy 1 group suggests a partial inclusion or an interaction of this ring with the MβCD cavity. However, in the methyl 1 group we observed that $\Delta\delta=-0.001$, which may be explained by the balance of opposing effects, one due to protection by the cavity and at the same time being more unprotected by the close proximity to oxygen atoms at the entrance.

The inclusion of the benzimidazole moiety was expected instead of the pyridinic moiety due to steric hindrance of methyl and methoxy pyridinic substituents. The interaction with the pyridinic fragment was found to be repulsive, as expected from the size of the fragment. On the other hand, the inclusion of the benzimidazole fragment has been demonstrated to be energetically favoured, but highly dependent on the orientation of the substituent methoxy group (41). The proposed structures for the inclusion complex formed between OME and each cyclodextrin are illustrated in Fig. 3.

Table I. Values of Apparent Stability Constant ($K_S \pm$ Standard Deviation) and OME Solubility with or without Inclusion Complex Formation

Inclusion complex	$S_0{}^a/(10^{-3}$ M)	$S_2{}^b/(10^{-3}$ M)	$D_2/(10^{-2})^c$	$K_S/(M^{-1})$
OME–βCD	3.366 ± 0.250	5.751 ± 0.093	16.889	56.931 ± 2.335
OME–MβCD		11.336 ± 0.118	19.350	77.397 ± 1.388

[a] OME solubility in borate buffer pH=10.
[b] OME solubility in CD solutions (13.2×10^{-3} M βCD and 42×10^{-3} M MβCD).
[c] Slopes of the phase solubility diagrams achieved in inclusion complexes.

Table II. ^{1}H Chemical Shifts Corresponding to MβCD in Free and Complexed State

Assignments	MβCD δ/(ppm)	OME:MβCD δ/(ppm)	$\Delta\delta$/(ppm)
H1	5.177	5.128	−0.049
H2	4.991	4.947	−0.044
H3	3.892	3.838	−0.054
H4	3.483	3.463	−0.020
H5	3.789	3.703	−0.086
H6	3.577	3.54	−0.037
Methyl-6′	3.307	3.252	−0.055

Figure 4 reports expansions of the ^{1}H NMR spectra of the OME aromatic region and methoxy groups in the absence of cyclodextrin (a) and presence of βCD (b) and MβCD (c). Complexation with cyclodextrins is frequently a dynamic process with the guest being in fast exchange between the free and bound states characterized by the absence of new peaks when the complex is formed. However, it was possible to observe the presence of new peaks in the ^{1}H NMR spectra of complexed OME relatively to the spectra of OME alone. This fact can be assigned to the presence of a sulphoxide group in the OME chemical structure acting as a chiral center. Normally, this drug is a racemate composed of the two isomers, *S* and *R*, in proportion 1:1 (42). Cyclodextrins, and its derivatives, have proved to be of great utility in analytical chemistry, especially in providing separations of positional and optical isomers (43). These spectra suggest that probably βCD and MβCD act as chiral selectors, promoting the separation of the two OME isomers. As we can appreciate (Fig. 4) in the absence of cyclodextrins it is impossible to distinguish the isomers by ^{1}H NMR experiments. The second source of diversity is that these compounds (*S* and *R* isomers) present tautomerism, illustrated by the modification of the methoxy group in the benzimidazole ring between two adjacent positions (5 and 6). This is the normal behaviour of all 5(6)-substituted benzimidazoles (44). In the ^{1}H NMR spectra it is suggested that the most abundant tautomer is the one with the methoxy group in position 6 of the benzimidazole ring but it is difficult to be totally confidant about this attribution since the δ for both tautomers are very similar.

Determination of the stoichiometry of the OME:cyclodextrin complexes was based on continuous variation method. Job plots $\Delta\delta\times$[OME] and $\Delta\delta\times$[CD] are presented in Figs. 5 and 6, respectively. For the sake of concision, only some protons, the most markedly affected, have been selected in the host and guest molecules. Such analysis reported the existence of a complex with a 1:1 stoichiometry, since the maximum was observed at r=0.5, within the range of the investigated concentrations. These results are in agreement with the phase solubility studies previously referred.

Table III. ^{1}H Chemical Shifts Corresponding to OME in Absence and in the Presence of MβCD

Assignments	OME δ/(ppm)	OME:MβCD δ/(ppm)	$\Delta\delta$/(ppm)
Ha	7.100	7.075	−0.025
Hb	6.785	6.749	−0.036
Hc	7.448	7.424	−0.024
Hd	8.067	8.077	0.010
Methoxy 1	3.444	3.419	−0.025
Methoxy 2	3.781	3.755	−0.026
Methyl 1	2.106	2.105	−0.001
Methyl 2	1.815	1.875	0.060

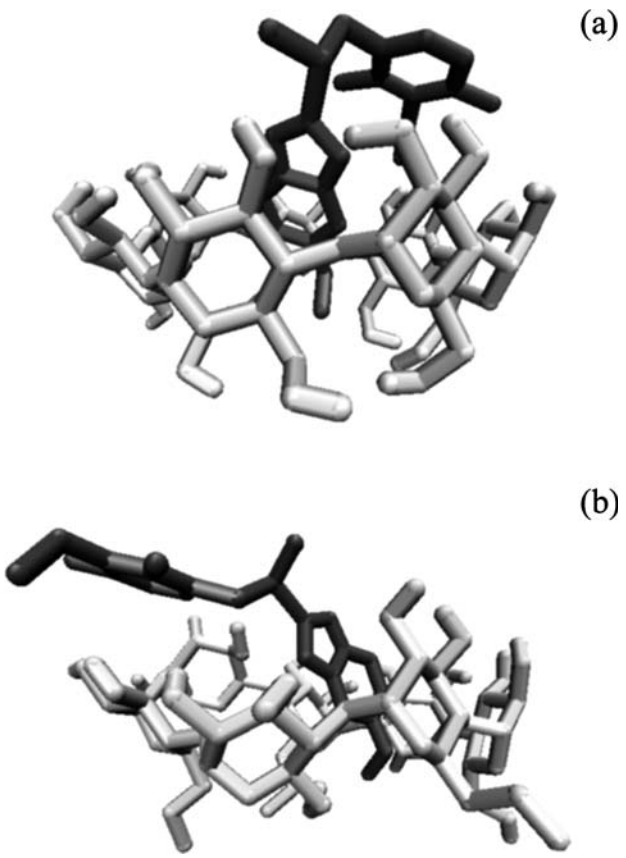

Fig. 3. Snapshots of the proposed inclusion complexes OME:βCD (a) and OME:MβCD (b). Omeprazole and cyclodextrin represented in *dark* and *light grey*, respectively.

ROESY Spectroscopy

Expansions of the ROESY spectrum of the OME:βCD and OME:MβCD complexes are reported in Fig. 7a and b. This bidimensional experiments show intermolecular cross-peaks between H-3 and H-5 protons of βCD/MβCD and aromatics protons of OME, namely, Ha, Hb and Hc. These observations are consistent with the occurrence of an inclusion of the OME benzimidazole fragment into the hydrophobic CDs cavities. The ROESY spectrum of the OME:MβCD complex, illustrated in Fig. 7b, shows the existence of more intense NOEs relatively to OME:βCD complex, in agreement with an higher K_S for the OME:MβCD complex (see Table I). The expansion of this ROESY shows more intense correlations between H-3 and Ha than with Hb/Hc suggesting that this proton must be close to the primary ring of the cyclodextrin cavity. On the other hand, correlations were intense between H-5 and the three aromatic protons (Ha, Hb and Hc), demonstrating a deeper inclusion of the benzimidazole moiety within the MβCD cavity through the wider end. In the case of βCD, correla-

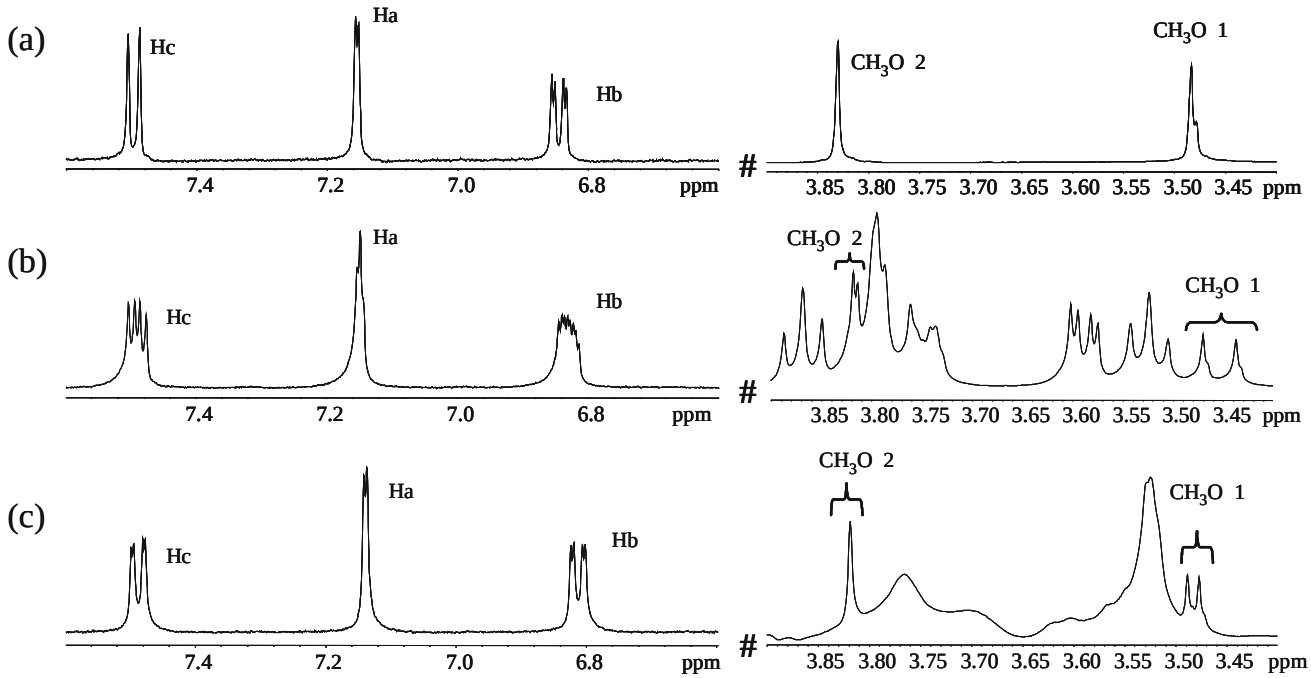

Fig. 4. Expansion of the ^{1}H NMR spectra of OME in the free state (a) and in the complexed formed with βCD (b) and with MβCD (c).

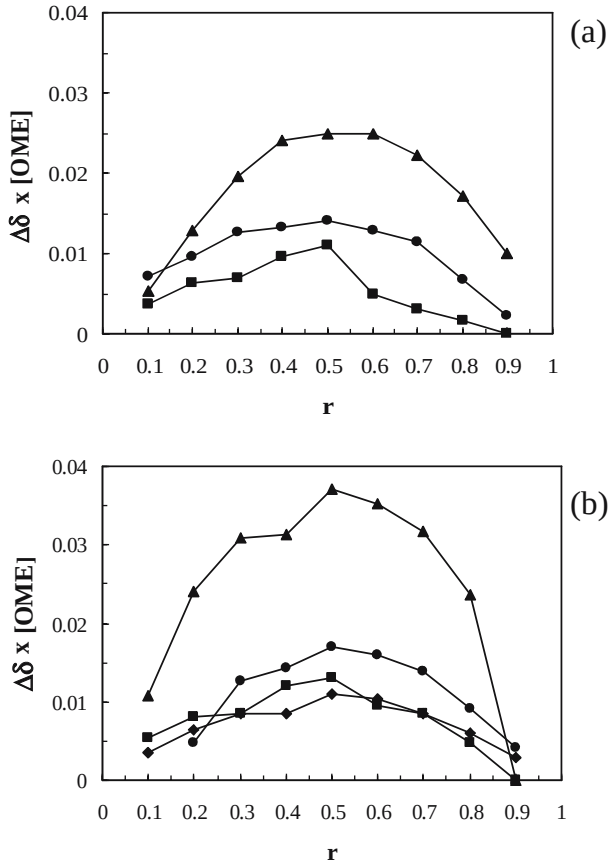

Fig. 5. Continuous variation plots for OME protons in βCD (a) and in MβCD (b) inclusion complex [protons of OME: (■) Hb, (●) Hd, (♦) methyl 1 and (▲) methyl 2].

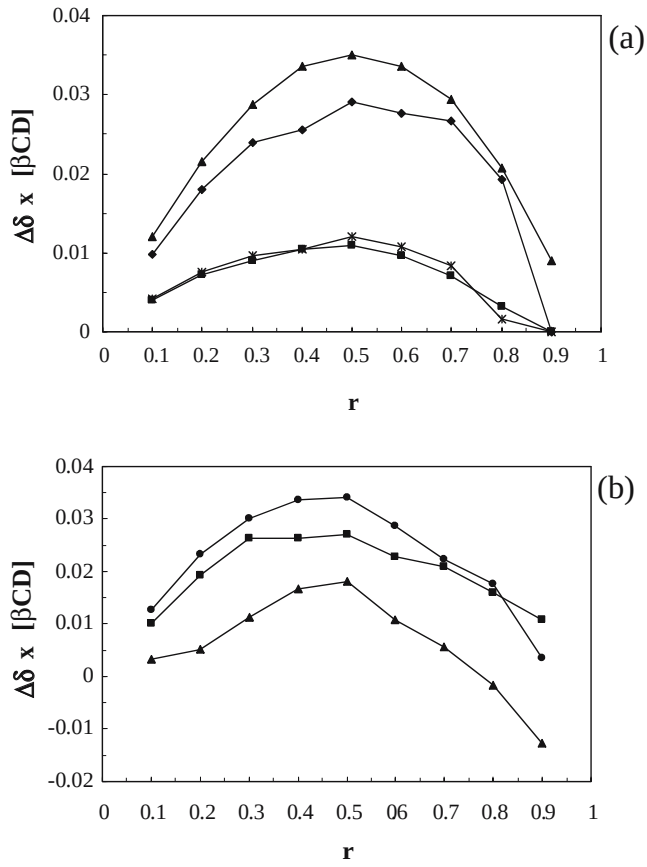

Fig. 6. Continuous variation plots for βCD (a) and in MβCD (b) in the inclusion complex with OME. [protons of βCD: (*) H1, (▲) H3, (■) H4 and (♦) H6; protons of MβCD: (▲) H3, (■) H5 and (♦) H6].

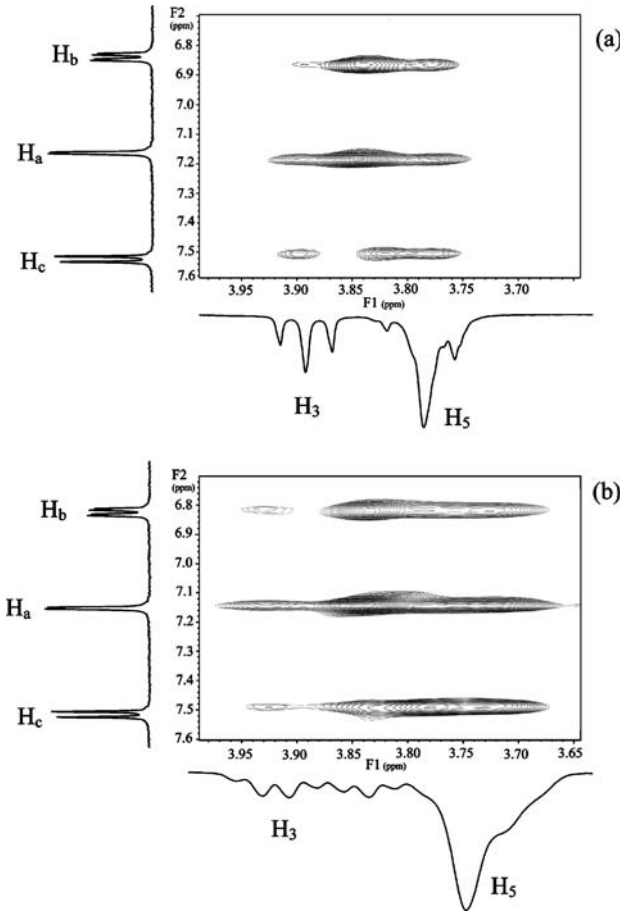

Fig. 7. ROESY expansions in the aromatic region of the drug for OME:βCD (a) and OME:MβCD (b) inclusion complexes.

tions were more intense between H-3 and Ha/Hc than with Hb and between H-5 and Ha/Hb than Hc.

The absence of NOE's between the protons of the cyclodextrins and protons of the OME pyridinic moiety, namely OME methoxy 1, suggests once more that for these groups the interaction is not very extensive. These results are in agreement with Δδ values from the ^{1}H NMR experiments.

Molecular Dynamics Simulation

Cyclodextrins in Solution

βCD molecules in gas phase have been observed by several authors to have a symmetrical conformation, similar to the one observed in the crystal. This is consistent with results of our calculations in gas phase, presented later. However, solvent interactions were observed, in this work, to be of great importance to the conformational behaviour of βCD and its methylated derivative.

Both βCD and MβCD were observed to have, when free in water, considerable conformational freedom. Figure 8 shows a rotation of the primary hydroxyl groups to the interior of the cavity. Both maxima corresponding to the O6 of the βCD and the non-substituted O6 of MβCD are shifted to small, similar distances. The substitution of the hydrogen by a methyl group in some of the O6 of MβCD apparently removes the possibility of these rings to rotate to the interior. This may be due to two reasons. On one hand, the bulky group, now present at the extremity of this small side chain, introduces steric restrictions to ring movement. On the other hand, the nonsubtituted groups retain the ability of forming hydrogen bonds amongst themselves when the ring is rotated, with the O6 position turned to the inside of the cavity. This ability is at least partially lost by the substitution creating an energetically inequality upon rotation between substituted and nonsubstituted groups. The ability of some rings to rotate with respect to the βCD plane, distorting considerably the geometry of the molecule, was previously reported (15).

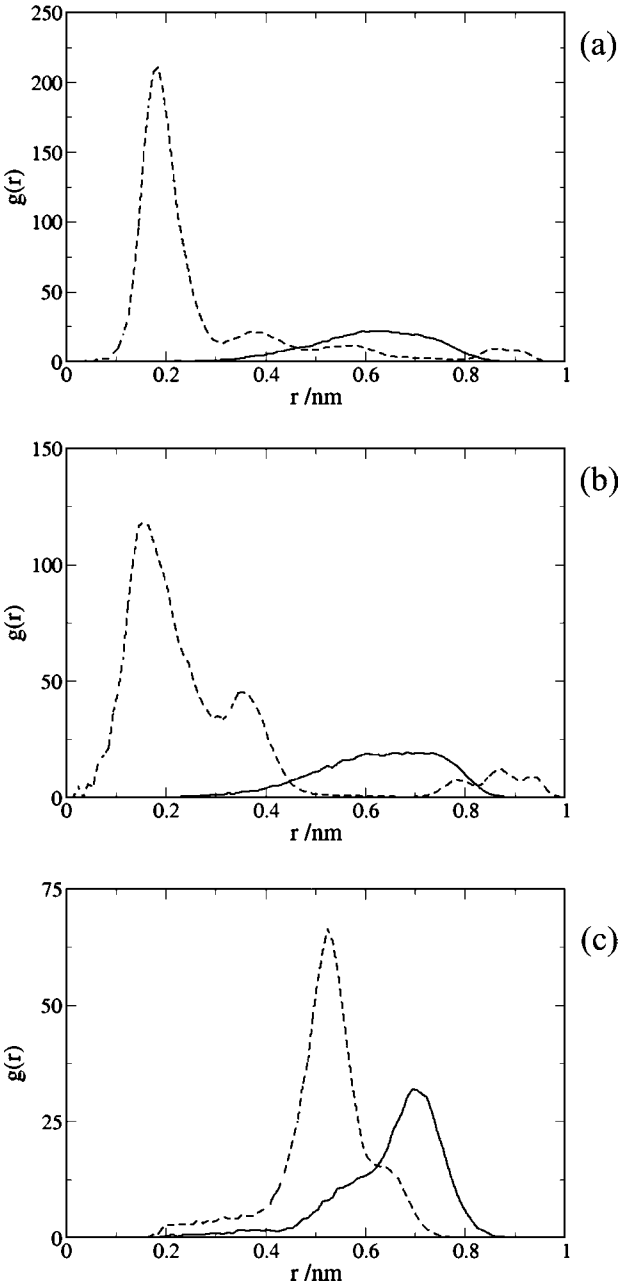

Fig. 8. Radial distribution functions for the O6 atoms around the center of mass of the group formed by all O1 atoms before (*full line*) and after (*dashed line*) ring distortion for the O6 in βCD (a), and the O6 of MβCD without (b) and with substituents groups (c).

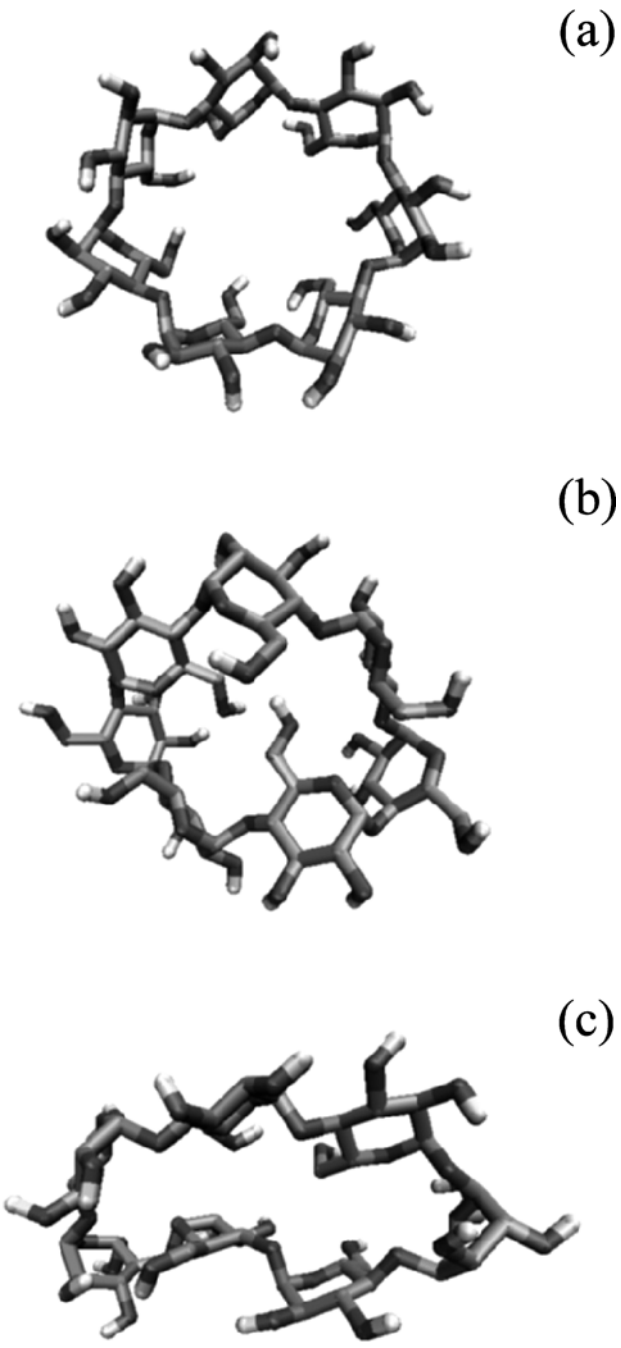

Fig. 9. Snapshots of the observed conformations of βCD in water (symmetric (a), distorted (b) and "collapsed" (c)). Hydrogen atoms in *white*, carbon atoms in *lighter grey* and oxygen atoms in *darker grey*.

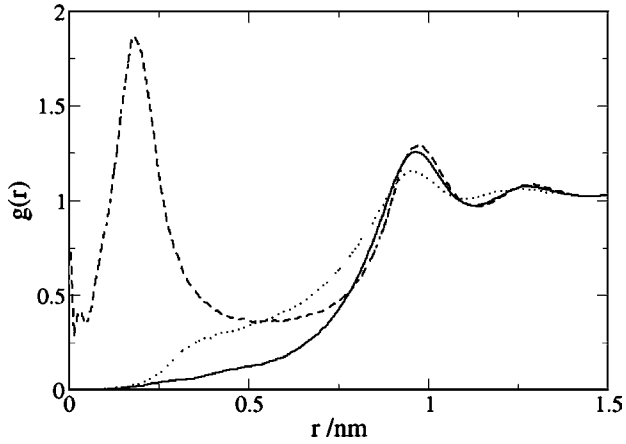

Fig. 10. Radial distribution functions of water around the center of mass of the group formed by all O1 atoms for the systems where OME is included inside βCD (*solid line*), βCD in the symmetric form (*dashed line*) and βCD in the distorted conformation (*dotted line*).

This conformational change, where primary hydroxyl groups rotate to the interior of the cavity (Fig. 9), corresponds to a substantial reduction of the area of contact with solvent water molecules originally in the interior of the cavity being expelled. The water release is clearly demonstrated in the radial distribution functions (RDFs) of Fig. 10. In this figure, the maximum present in the RDF corresponding to the water molecules in the interior of the cavity of the symmetrical conformation (with $r < 4$ Å, approximately) completely disappears in the RDF obtained for conformations where the ring adopted a distorted conformation. Note that the probability of the different functions at intermediate distances range (0.4 nm $< r <$ 1.0 nm) is of difficult analysis since it is affected by the lack of spherical symmetry around the reference point. In the distorted conformation, it is visible a decrease in the probability given by the first maximum corresponding to the disruption of the free water structure in the proximity of the cyclodextrin.

Cyclodextrin may also achieve other less frequent conformations in which the water molecules in the cavity are expelled by a "collapse" of the cyclodextrin ring (Fig. 9c), a situation already known to occur in α-cyclodextrin molecules in aqueous solutions (45) but to our knowledge not yet observed for βCD.

The heat of formation, ΔH_f, for the initial and distorted conformations obtained from GAMESS at the semi-empirical pm3 level in gas phase are presented in Table IV. These values indicate that the most stable conformation in gas phase for both cyclodextrins is the one where the cavity is accessible to the solvent. We may attribute the changes from the most symmetrical to distorted conformations to solvent interaction effects. The collapsed conformations were not found for the MβCD during the simulation run.

The change in conformation leads to the occupation of the cavity where the OME would enter forming the complex by the primary hydroxyl groups and thereby may influence the complex formation constant. However, it has not been possible to determine definitely the relative probability of

Table IV. Heat of Formation, ΔH_f, of the Optimized Gas Phase Structures of Initial and Final Conformations of βCD and MβCD in Aqueous Solution (in kcal mol^{-1})

	Initial conformation	Distorted conformation	"Collapsed" conformation
βCD	−1449.86	−1441.15	−1429.7
MβCD	−1432.71	−1419.01	

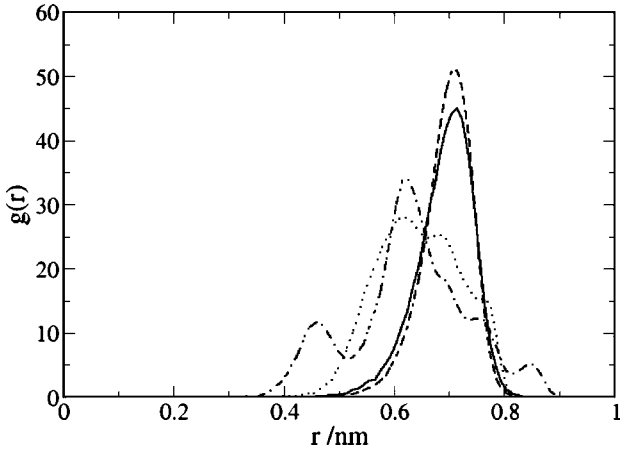

Fig. 11. Radial distribution functions for the O2 around the center of mass of the group formed by the O1 atoms of cyclodextrins for the initial (*solid* and *dashed lines* for βCD and MβCD, respectively) and distorted type conformations (*dotted* and *dash-dotted lines* for βCD and Mβcd, respectively).

occurrence of each conformation by Molecular Dynamics simulation nor if the cavity is reformed concomitant with inclusion.

The presence of substituents in the narrow entrance of cyclodextrin has also some influence on the dimensions of the wider entrance. In Fig. 11 are represented the RDF for the atoms O2 of βCD and MβCD for the initial and distorted conformations. No significant difference is observed in the more symmetric conformations, with both RDFs presenting a single maximum at $r \approx 0.7$ nm. This obviously reflects the radial symmetry of the molecule. At the same time this maximum provides an estimate of the diameter of the wider entrance of approximately 1.4 nm. In the distorted conformation the higher maximum for βCD is shifted to smaller r values and two other "shoulders" appear. The increased number of maxima and the shift in the position of the higher maxima indicate a considerable distortion of the ring. It becomes more elongated with reduction on the diameter of the wider entrance. The differences between the symmetrical and distorted conformations are even more pronounced in the case of MβCD. It is interesting to note that when comparing the results for the distorted βCD and MβCD, the maxima and the "shoulders" appear at similar distances from the center of mass considered, but in the latter two additional maxima appear. These may be directly related to the presence of methyl groups in the opposite side of the ring. The entrance to the cavity in this case is even more stretched, apparently, with a diameter in one direction of $r \approx 1.7$ and in another direction of $r \approx 0.9$ nm.

Inclusion Complexes

Figure 12 shows the distribution of distances between the center of mass of the benzene ring, the center of mass of the group formed by atoms *e* and *f* and the center of mass of the OME imide part to the center of mass of the group formed by all O1 atoms of the cyclodextrins. For the βCD case, we can see that there is a sequential increase in the distance at which the maximum of the distributions appear. From the first to the second maximum as well as from the second to the third, the maxima are separated by approximately 1 Å, which is about the distance of the points considered in the structure of the molecule. In Fig. 12b we have a slightly different situation. The second and third distributions present a shift to smaller distances while the first shows a shift to larger distances. Also, in this case, the maxima of the first and second curves are essentially positioned at the same distance from the center of mass of the group formed by the O1 atoms of the cyclodextrin. The distance between the two maxima is smaller than the distance between the two corresponding points in the OME molecule. An interpretation of these results leads to the conclusion that OME penetrates more deeply into the MβCD cavity than into βCD. In the OME:βCD complex the center of mass of the group formed by the O1 of the cyclodextrin is situated between position *b* and *a* while in the MβCD it is located between the center of mass of the benzene ring and the center of mass of the group formed by *e* and *f*. A more profound inclusion in MβCD is in agreement with experimental results shown in previous sections (phase solubility studies and ROESY experiments).

The inclusion of OME into the cyclodextrins, with removal of the water molecules from the interior of the cavity (Fig. 10), influences the conformational freedom of the drug. Figure 13 shows the distribution for the values of the angle formed by the O (in methoxy 2), S and C (methyl 1) atoms when complexed to each cyclodextrin and when free in solution. It is clearly visible that the OME molecule displays

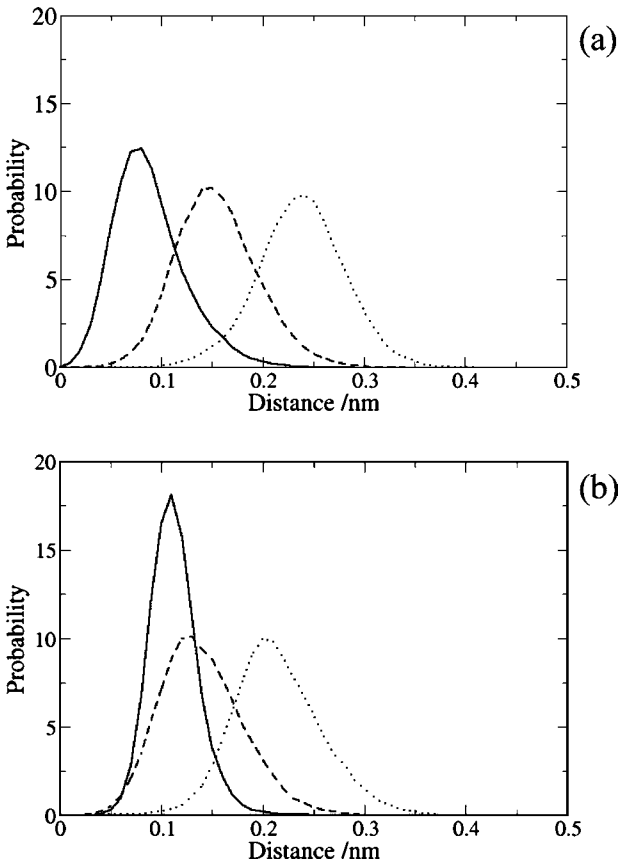

Fig. 12. Distance distribution from the center of mass of the benzene (*full line*), center of mass of the atoms *e* and *f* (*dashed line*) and center of mass of the imide part of OME (*dotted line*) to the center of mass of the group formed by the O1 of βCD (a) and MβCD (b).

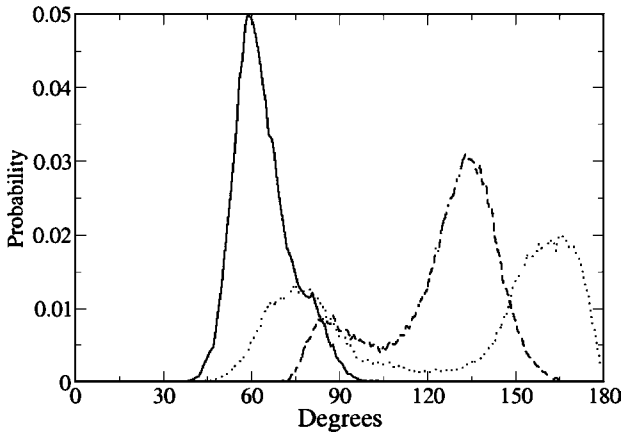

Fig. 13. Angle distribution for the angle formed by the O (methoxy 2), S and C (methyl1) atoms when OME is complexed with βCD (*full line*), with MβCD (*dashed line*) and free in solution (*dotted line*).

a tendency to be more stretched when complexed with the MβCD than when it is complexed with the βCD. In the latter case, the distribution presents a single maximum located well below 90° reflecting a preferential bent conformation, probably originated by solvent interaction effects. A certain degree of conformational freedom is still preserved in the inclusion with MβCD. In this case, the distribution still shows two maxima, as in the case where OME is free in solution, but the range of the experienced angles is more restrained and a considerable difference in probability between small and large angles is seen with higher probability for the latter. This indicates a small restraining action of MβCD on the conformation of OME.

The nearest-neighbor distances from methoxy atoms to several reference atoms of the cyclodextrin for the inclusion complexes structures are presented on Fig. 14. The interaction behavior between the OME methoxy 2 group and the selected reference cyclodextrin atoms (O2, O3 and O6) is very similar in OME:βCD and OME:MβCD (Fig. 14b and d). The methoxy 2 group is, in both cases, situated closer to O6 atoms than to O2 or O3 due to the very deep inclusion into the cavity. In the OME:MβCD case there is a small shift of the nearest-neighbor distances from O2 and O3 to methoxy 2 to smaller distances (Fig. 14d). The corresponding distributions concerning methoxy 1 (Fig. 14a and c) present more visible differences between the two complexes. The distance distribution from methoxy 1 to O6 in OME:βCD (Fig. 14a) presents a larger dispersion of values which can be related to an apparent larger mobility of the OME in the interior of the cavity and/or bending ability when compared to the OME:MβCD complex (Fig. 14c). The methoxy 1-O6 distance distribution for the OME:MβCD presents a shift of the

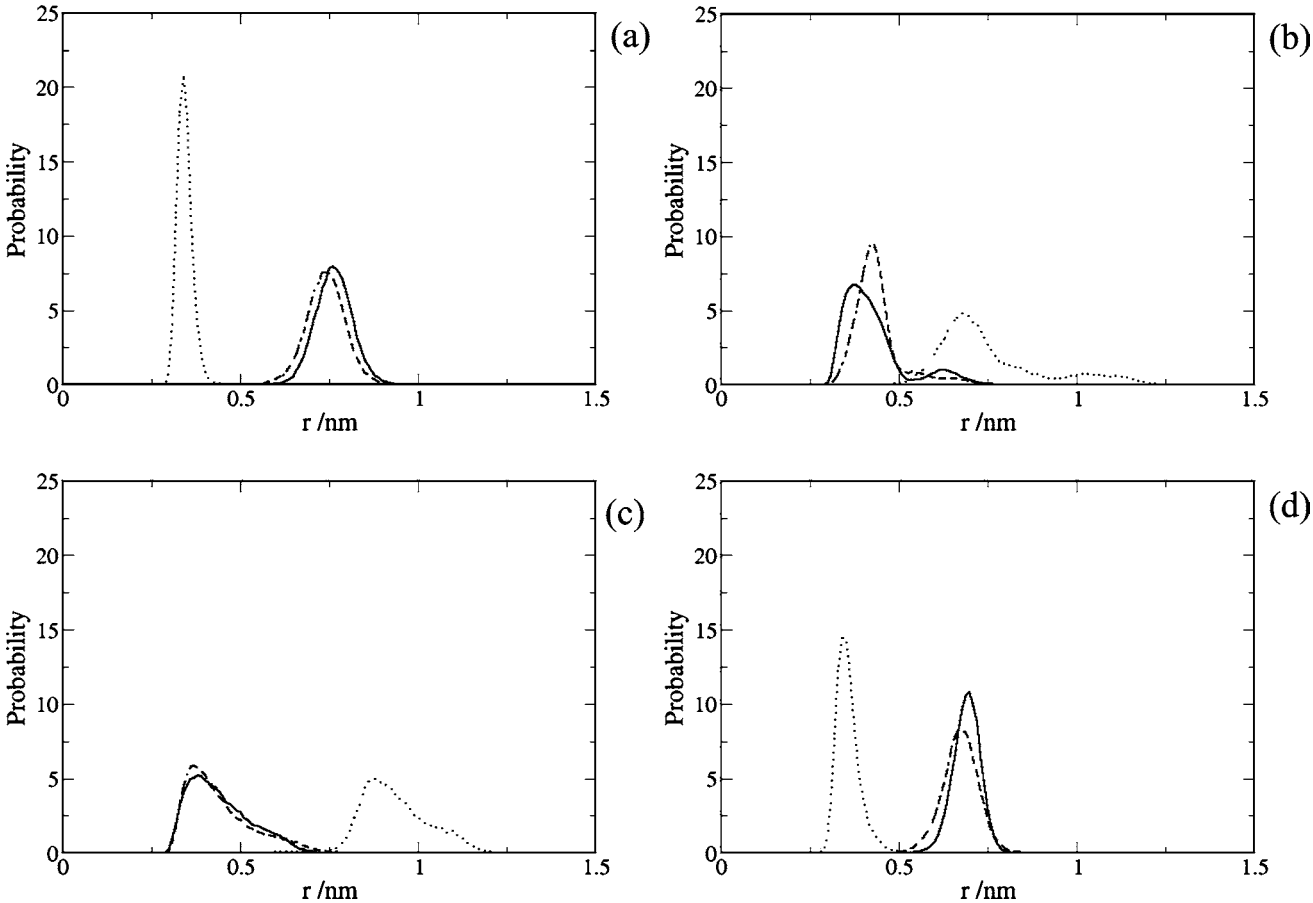

Fig. 14. Nearest-neighbor distance distribution of the positions methoxy 1 (*left*) and methoxy 2 (*right*) to the O2 (*full line*) O3 (*dashed line*) and O6 (*dotted line*) of the βCD (*top row*) and MβCD (*bottom row*).

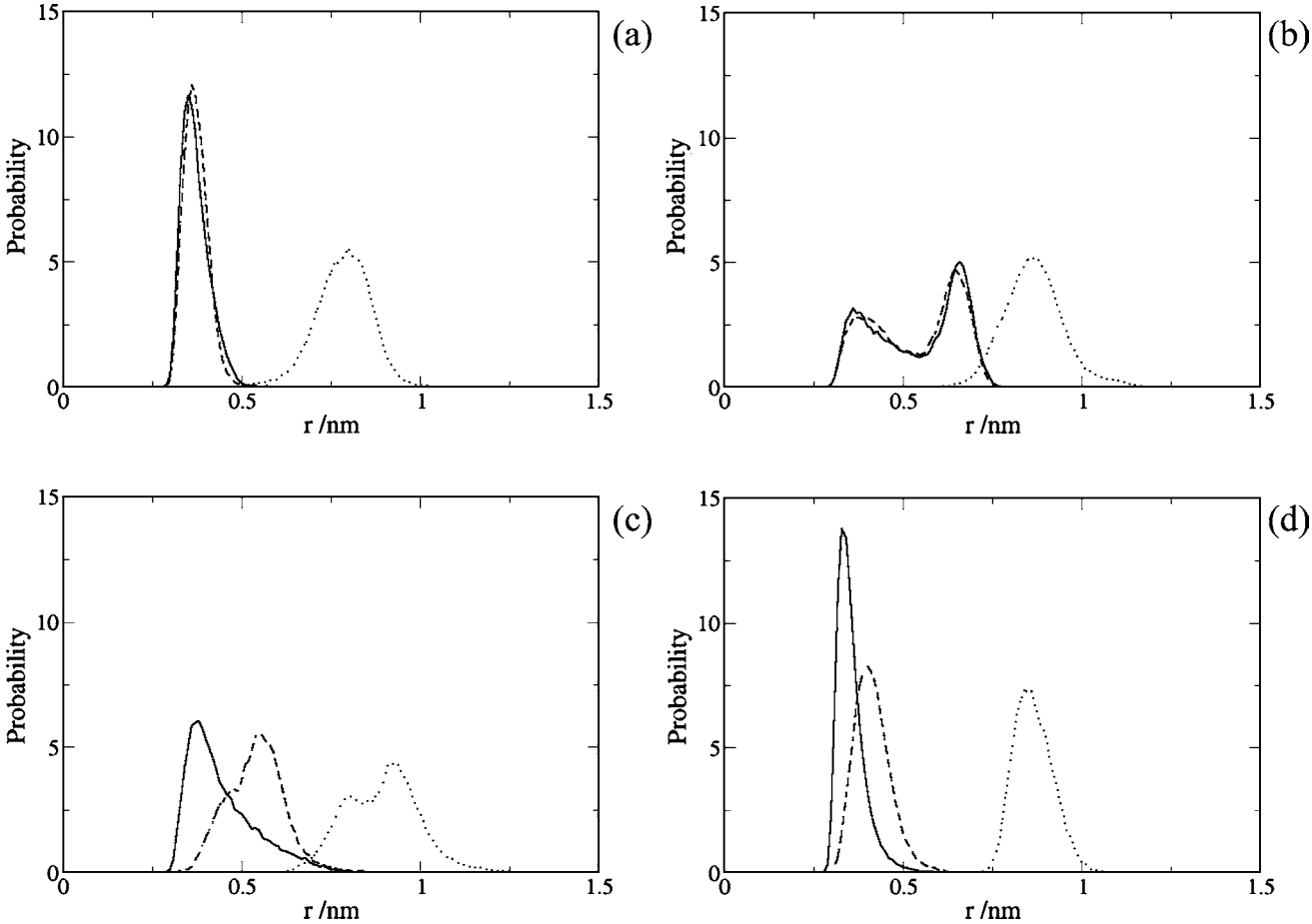

Fig. 15. Nearest-neighbor distance distribution of the positions methyl1 (*left*) and methyl2 (*right*) to the O2 (*full line*) O3 (*dashed line*) and O6 (*dotted line*) of the βCD (*top row*) and MβCD (*bottom row*).

maximum to larger distances. In respect to the distances from methoxy 1 to the atoms in the cyclodextrin wider entrance (Fig. 14a), the methoxy 1 is closer to the O2, which is located in the interior of the cavity, than to the O3. This difference is not observed in the case of OME:MβCD.

The maximum in the distance distribution of the closest reference atoms of the cyclodextrins to methoxy 1 and methoxy 2 are located at similar positions (Fig. 14a and b and Fig. 14c and d). However, this position corresponds to O2 in the methoxy 1 case while it corresponds to O6 in the methoxy 2 case. This explains the significant difference in $\Delta\delta$ values for methoxy 2 upon methylation of the cyclodextrin. The $\Delta\delta$ values of methoxy 1 remain unchanged, as mentioned on a previous section (see Table III) since chemical environment around methoxy 1 does not suffer significant changes with methylation. However the introduction of methyl groups on the O6 position disables the possibility of formation of the same number of hydrogen bonds as with βCD and thus leads to a more negative $\Delta\delta$ of methoxy 2 upon methylation, and similar to the one observed for methoxy 1.

In the panels of Fig. 15 we present the nearest-neighbor distance distributions between the methyl groups (1 and 2) of OME and the oxygens in positions 2, 3 and 6 of both cyclodextrins. It is observed that when OME is included in CD (Fig. 15a and b), both methyl groups present similar distance distributions to O2 and O3. In the case of methyl 2 two maxima appear for both distributions (Fig 15b). On the OME:MβCD case (Fig. 15c and d) only one single maxima appears for each distribution. In the inclusion with MβCD the closest cyclodextrin reference atom is always the O2, with the distribution of methyl 2 (Fig. 15d) having clearly a smaller dispersion. This is in agreement with the results obtained in the experimental part of this work, with both methyl groups being more closely located to the atoms situated inside the cavity of MβCD. It is also observable that in all cases the distance distribution to O6 has its maximum for distances larger than the ones observed for O2 and O3.

CONCLUSION

The complex formation in aqueous solution between OME and MβCD was confirmed by phase solubility studies, ^{1}H NMR experiments and Molecular Dynamics. The stoichiometry of 1:1 of the complex was determined by phase solubility studies and confirmed by the continuous variation method (Job plot studies). According to the NMR results, supported by Molecular Dynamics, the complex is formed by the inclusion of the benzimidazole part of the OME into the cyclodextrin cavity. The complexes formed with MβCD were observed to have a larger K_S, which may be

explained by two simultaneous effects. On one hand, ROESY experiments and Molecular Dynamics simulations indicate that OME is more deeply included in the MβCD cavity. On the other hand simulations studies showed that methylation has an effect on the conformational behaviour of the cyclodextrins in aqueous solutions that may to some extent alter the probability of formation of the complex. The solubility of OME is increased by complexation with both cyclodextrins, but MβCD was observed to be a more efficient agent by forming more stable 1:1 complexes with the drug.

ACKNOWLEDGMENTS

This work was financially supported by a grant (Praxis SFRH/BD/19175/2004) from FCT (Fundação para a Ciência e a Tecnologia, Portugal). The authors would like to thank the technical assistance of Tiago Alves and Patricia Nunes (Departamento de Bioquímica, Faculdade de Ciências e Tecnologia, Universidade de Coimbra) in the acquisition of NMR spectra. We also acknowledge Belmac Laboratory, S.A. (Barcelona, Spain) for the kindly donation of OME and Roquette (Lestrem, France) for their support providing βCD and MβCD.

REFERENCES

1. C. W. Howden. Clinical pharmacology of omeprazole. *Clin. Pharmacokinet.* **20**:38–40 (1990).
2. N. Sarisuta, T. Tourtip, and S. Chuarcharoern. Chemical stability and mechanism of degradation of omeprazole. *Thai. J. Pharm. Sci.* **22**:81–88 (1998).
3. L. Marzocchi, J. R. Moyano, A. Rossi, P. Muñoz, M. J. Arias, and F. Giordano. Current status of ATP-ase proton pump inhibitor complexation with cyclodextrins. *Biolog. J. Armenia.* **53**:176–193 (2001).
4. M. E. Davis and M. E. Brewster. Cyclodextrin-based pharmaceutics: past, present and future. *Nat. Rev. Drug Discov.* **3**:1023–1035 (2004).
5. E. M. Martin Del Valle. Cyclodextrins and their uses: a review. *Process Biochem.* **39**:1033–1046 (2004).
6. N. Dupuy, D. Barbry, M. M. S. Bria, M. L. Vrielynck, and J. Kister. ^{1}H NMR study of inclusion compounds of phenylurea derivatives in β-cyclodextrin. *Spectrochim. Acta A.* **61**:1051–1057 (2005).
7. C. A. Ventura, I. Giannone, D. Paolino, V. Pistarà, A. Corsaro, and G. Puglisi. Preparation of celecoxib-dimethyl-β-cyclodextrin inclusion complex: characterization and *in vitro* permeation study. *Eur. J. Med. Chem.* **40**:624–631 (2005).
8. T. Higuchi and A. K. Connors. Phase-solubility techniques. In C. N. Reill (ed.), *Advances in Analytical Chemistry and Instrumentation*, Wiley, New York, 1965, pp. 117–212.
9. R. Challa, A. Ahuja, J. Ali, and R. K. Khar. Cyclodextrins in drug delivery: an updated review. *AAPS Pharm. Sci. Tech.* **6**:E329–E357 (2005).
10. C. M. Fernandes, R. A. Carvalho, S. Pereira da Costa, and F. J. B. Veiga. Multimodal molecular encapsulation of nicardipine hydrochloride by β-cyclodextrin, hydroxypropyl-β-cyclodextrin and triacetyl-β-cyclodextrin in solution. Structural studies by ^{1}H NMR and ROESY experiments. *Eur. J. Pharm. Sci.* **18**:285–296 (2003).
11. D. Salvatierra, C. Jaime, A. Virgilli, and F. Sánchez-Ferrando. Determination of the inclusion geometry for the β-cyclodextrin/benzoic acid complex by NMR and molecular modeling. *J. Org. Chem.* **61**:9578–9581 (1996).
12. S. M. Ali, F. Asmat, and A. Maheshwari. NMR spectroscopy of inclusion complex of D-(-)-chloramphenicol with β-cyclodextrin in aqueous solution. *Il Farmaco.* **59**:835–838 (2004).
13. A. Bernini, O. Spiga, A. Ciutti, M. Scarselli, G. Bottoni, P. Mascagni, and N. Niccolai. NMR studies of the inclusion complex between β-cyclodextrin and paroxetine. *Eur. J. Pharm. Sci.* **22**:445–450 (2004).
14. N. E. Polyakov, T. V. Leshina, E. O. Hand, A. Petrenko, and L. D. Kispert. β-Ionone cyclodextrins inclusion complexes: ^{1}H NMR study and photolysis. *J. Photochem. Photobiol. A—Chem.* **161**:261–267 (2004).
15. B. Manunza, S. Deiana, M. Pintore, and C. Gessa. Structure and internal motion of solvated beta-cyclodextrine: a molecular dynamics study. *J. Mol. Struct.* **419**:133–137 (1997).
16. E. B. Starikov, K. Bräsicke, E. W. Knapp, and W. Saenger. Negative solubility coefficient of methylated cyclodextrins in water: A theoretical study. *Chem. Phys. Lett.* **336**:504–510 (2001).
17. L. Lawtrakul, H. Viernstein, and P. Wolschan. Molecular dynamics simulations of β-cyclodextrin in aqueous solution. *Int. J. Pharm.* **256**:33–41 (2003).
18. B. Jursic, Z. Zdravkovski, and A. D. French. Molecular modeling methodology of β-cyclodextrin inclusion complexes. *J. Mol. Struct.* **336**:113–117 (1996).
19. E. Alvira, J. A. Mayoral, and J. I. García. Molecular modelling study of β-cyclodextrin inclusion complexes. *Chem. Phys. Lett.* **271**:178–184 (1997).
20. M. T. Faucci, F. Melani, and P. Mura. Computer-aided molecular modeling techniques for predicting the stability of drug–cyclodextrin inclusion complexes in aqueous solutions. *Chem. Phys. Lett.* **358**:383–390 (2002).
21. W. Chen, C. E. Chang, and M. K. Gilson. Calculation of cyclodextrin binding affinities: energy, entropy, and implications for drug design. *Biophys. J.* **87**:3035–3049 (2004).
22. U.S.P. XXVIII. *The United States Pharmacopoeia* 25th United States Pharmacopeial Convention Inc., Rockville, 2005.
23. L. Ribeiro, R. Carvalho, D. C. Ferreira, and F. J. B. Veiga. Multicomponent complex formation between vinpocetine, cyclodextrins, tartaric acid and water soluble polymers monitored by NMR and solubility studies. *Eur. J. Pharm. Sci.* **24**:1–13 (2005).
24. H. J. C. Berendsen, D. van der Spoel, and R. van Drunen. GROMACS: A message-passing parallel molecular dynamics implementation. *Comput. Phys. Commun.* **91**:43–56 (1995).
25. E. Lindahl, B. Hess, and D. van der Spoel. GROMACS 3.0: A package for molecular simulation and trajectory analysis. *J. Mol. Mod.* **7**:306–317 (2001).
26. G. J. Kleywegt and T. A. Jones. Databases in protein crystallography. *Acta Crystallogr. Sect. D—Biol. Crystallogr.* **D54**:1119–1131 (1998).
27. C. K. Lee, E. J. Kim, and J. H. Jun. Determination of relative reactivities of free hydroxyl groups in β-cyclodextrin, amylose, and cellulose by Reductive Cleavage Method. *Bull. Korean Chem. Soc.* **20**:1153–1158 (1999).
28. A. W. Schuettelkopf and D. M. F. van Aalten. PRODRG—a tool for high throughput crystallography of protein–ligand complexes. *Acta Crystallogr. Sect. D—Biol. Crystallogr.* **D60**: 1355–1363 (2004).
29. A. Brändström, N. A. Bergman, I. Grundevik, S. Johansson, L. Tekenbergs-Hjelte, and K. Ohlson. Chemical reactions of omeprazole and omeprazole analogues. III. Protolytic behaviour of compounds in the omeprazole system. *Acta Chem. Scand.* **43**:569–576 (1989).
30. R. Yang, S. G. Schulman, and P. J. Zavala. Acid–base chemistry of omeprazole in aqueous solutions. *Anal. Chim. Acta.* **481**: 155–164 (2003).
31. M. W. Schmidt, K. K. Baldridge, J. A. Boatz, S. T. Elbert, M. S. Gordon, J. H. Jensen, S. Koseki, N. Matsunaga, K. A. Nguyen, S. J. Su, T. L. Windus, M. Dupuis, and J. A. Montgomery. General atomic and molecular electronic-structure system. *J. Comput. Chem.* **14**:1347–1363 (1993).
32. U. Essman, L. Perela, M. L. Berkowitz, T. Darden, H. Lee, and L. G. Pedersen. A smooth particle mesh ewald method. *J. Chem. Phys.* **103**:8577–8592 (1995).

33. S. Miyamoto and P. A. Kollman. Settle: An analytical version of the shake and rattle algorithms for rigid water models. *J. Comput. Chem.* **13**:952–962 (1992).
34. H. J. C. Berendsen, J. P. M. Postma, A. DiNola, and J. R. Haak. Molecular dynamics with coupling to an external bath. *J. Chem. Phys.* **81**:3684–3690 (1984).
35. B. Hess, H. Bekker, H. J. C. Berendsen, and J. G. E. M. Fraaije. LINCS: A linear constraint solver for molecular simulations. *J. Comput. Chem.* **18**:1463–1472 (1997).
36. T. Loftsson, D. Hreinsdóttir, and M. Másson. Evaluation of cyclodextrin solubilization of drugs. *Int. J. Pharm.* **302**:18–28 (2005).
37. K. Hanna, C. H. Brauer, and P. Germain. Cyclodextrin-enhanced solubilization of pentachlorophenol in water. *J. Environ. Manag.* **71**:1–8 (2004).
38. A. Zornoza, C. Martín, M. Sánchez, and A. Piquer. Inclusion complexation of glisentide with α-, β- and γ-cyclodextrins. *Int. J. Pharm.* **169**:239–244 (1998).
39. T. Loftsson, B. J. Ólafsdóttir, H. Frioriksdóttir, and S. Jónsdóttir. Cyclodextrin complexation of NSAIDs physicochemical characteristics. *Eur. J. Pharm. Sci.* **1**:95–101 (1993).
40. Y. Inoue. NMR studies of the structure and properties of cyclodextrins and their inclusion complexes. *Annu. Rep. NMR Spectrosc.* **27**:59–69 (1993).
41. S. Braga, P. Ribeiro-Claro, M. Pillinger, I. Gonçalves, A. Fernandes, F. Pereira, C. Romão, P. Correia, and J. Teixeira-Dias. Interactions of omeprazole and precursors with β-cyclodextrin host molecules. *J. Incl. Phenom. Macrocycl. Chem.* **47**:47–52 (2003).
42. J. J. Berzas Nevado, G. Castañeda Peñalvo, and R. M. Rodríguez Dorado. Method development and validation for the separation and determination of omeprazole enantiomers in pharmaceutical preparations by capillary electrophoresis. *Anal. Chim. Acta.* **533**:127–133 (2005).
43. P. S. Bonato and F. O. Paias. Enantioselective analysis of omeprazole in pharmaceutical formulations by chiral high-performance liquid chromatography and capillary electrophoresis. *J. Braz. Chem. Soc.* **15**:318–323 (2004).
44. R. M. Claramunt, C. López, I. Alkorta, J. Elguero, R. Yang, and S. Schulman. The tautomerism of omeprazole in solution: a H and C NMR study. *Magn. Reson. Chem.* **42**:712–714 (2004).
45. J. Szejtli. Introduction and general overview of cyclodextrin chemistry. *Chem. Rev.* **98**:1743–1753 (1998).